

吡嗪酰肼配体 Cu(II)/Ni(II)配合物的合成、晶体结构及 DNA 结合性质

王碗碗¹ 王元^{*1} 张玲¹ 宋雨飞¹ 吴伟娜^{*1} 陈忠²

(¹河南理工大学化学化工学院,河南省煤炭绿色转化重点实验室,焦作 454000)

(²江西科技师范大学材料与机电学院,南昌 330013)

摘要: 合成并通过单晶衍射、元素分析及红外光谱表征了配合物 $[\text{Ni}(\text{L})(\text{HL})](\text{SO}_4)_{0.5} \cdot 3\text{CH}_3\text{OH}$ (**1**)和 $[\text{Cu}_2(\text{L})_2\text{SO}_4] \cdot 1.5\text{CH}_3\text{OH}$ (**2**)的结构(HL为3-甲基-2-乙酰吡嗪苯甲酰肼)。单晶衍射实验结果表明,在配合物**1**中,Ni(II)中心离子与2个酰肼配体的[ONN]配位原子组配位,形成扭曲的八面体配位构型;**2**的最小非对称单元中含有1个独立的双核Cu(II)配合物分子,它的2个Cu(II)中心由2个酰肼配体中的2个O原子桥联。每个Cu(II)离子还与L⁻配体中的2个氮原子和 $\eta_2\text{-SO}_4^{2-}$ 阴离子中的1个O原子配位,拥有扭曲的四方锥配位构型。此外,荧光光谱表明配合物和DNA的结合能力强于配体。

关键词: 酰肼; Cu(II)配合物; DNA结合; Ni(II)配合物; 吡嗪

中图分类号: O614.121; O614.81+3 文献标识码: A 文章编号: 1001-4861(2019)03-0563-06

DOI: 10.11862/CJIC.2019.037

Syntheses, Crystal Structures and DNA-Binding Properties of Cu(II)/Ni(II) Complexes with Acylhydrazone Ligand Bearing Pyrazine Unit

WANG Wan-Wan¹ WANG Yuan^{*1} ZHANG Ling¹ SONG Yu-Fei¹ WU Wei-Na^{*1} CHEN Zhong²

(¹College of Chemistry and Chemical Engineering, Henan Key Laboratory of Coal Green Conversion, Henan Polytechnic University, Jiaozuo, Henan 454000, China)

(²School of Materials and Mechanical and Electrical Engineering, Jiangxi Science and Technology Normal University, Nanchang 330013, China)

Abstract: Two complexes, namely $[\text{Ni}(\text{L})(\text{HL})](\text{SO}_4)_{0.5} \cdot 3\text{CH}_3\text{OH}$ (**1**) and $[\text{Cu}_2(\text{L})_2\text{SO}_4] \cdot 1.5\text{CH}_3\text{OH}$ (**2**) (HL=3-methyl-2-acetylpyrazine benzoylhydrazone) have been synthesized and characterized by single crystal X-ray diffraction, elemental analysis and IR spectroscopy. X-ray diffraction analysis results showed that in complex **1**, the center Ni(II) ion with a distorted octahedron geometry is surrounded by two acylhydrazones with [ONN] donor set. However, complex **2** contains one discrete dimeric Cu(II) molecule in the unit cell, in which two Cu(II) ions were doubly bridged by two O atoms from two independent acylhydrazone ligands. Each of the Cu(II) ions is also coordinated by two N atoms from one L⁻ ligand and one O atom from the $\eta_2\text{-SO}_4^{2-}$ anion, thus giving a distorted square pyramidal coordination geometry. Moreover, the fluorescence spectra indicated that the interaction of the complexes to DNA is stronger than that of the ligand HL. CCDC 1876785: **1**; 1876789: **2**.

Keywords: acylhydrazone; Cu(II) complex; DNA-binding; Ni(II) complex; pyrazine

收稿日期:2018-11-05。收修改稿日期:2018-11-27。

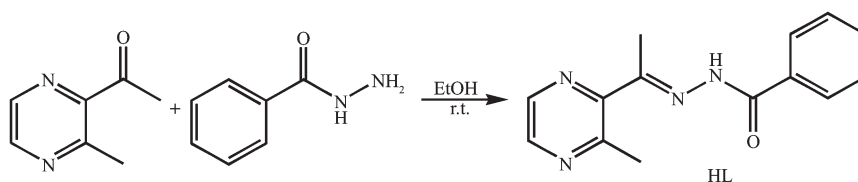
国家自然科学基金(No.21001040),河南省自然科学基金(No.182300410183,162300410011),江西省自然科学基金(No.20181BAB206011),河南省教育厅高等学校重点科研基金(No.19A150001),江西省教育厅科学技术研究项目(No.GJJ170665),河南理工大学校内基金(No.T2018-3,J2015-4)和江西科技师范大学校内基金(No.2015QNBjRC006)资助。

*通信联系人。E-mail:wangyuan08@hpu.edu.cn,wuwn08@hpu.edu.cn;会员登记号:S06N6704M1112(吴伟娜)。

Schiff bases and their metal complexes have been widely used in medical fields such as anticancer, antibacterial, and antiviral drugs^[1-2]. Generally, the presence of a heterocyclic ring in the synthesized Schiff bases plays a major role in extending their pharmacological properties^[3]. Particularly, pyrazine-containing thiosemicarbazone has been extensively investigated as potential anticancer agents^[4], because pyrazine is a vital nitrogen heterocyclic compound with various biological activities and a key structural unit for the drug design^[4-6]. However, acylhydrazones bearing pyrazine unit, as their structural analogs,

received much less attention^[4,7-8].

Our previous work has showed that 2-acetopyrazine benzoylacylhydrazone could form stable complexes with transition metal ions, such as Cu(II), Ni(II) and Zn(II)^[5]. It is noted that the biological activities of acylhydrazones often show a high dependence on their substituent^[9]. In this regard, we chose 2-aceto-3-methylpyrazine as the starting material for the formation of benzoylacylhydrazone ligand HL (Scheme 1). In this paper, the structures and DNA-binding properties of its Ni(II)/Cu(II) complexes have been discussed in detail.



Scheme 1 Synthetic route of HL

1 Experimental

1.1 Materials and measurements

Solvents and starting materials for synthesis were purchased commercially and used as received. Elemental analysis was carried out on an Elemental Vario EL analyzer. The IR spectra ($\nu=4\ 000\sim 400\text{ cm}^{-1}$) were determined by the KBr pressed disc method on a Bruker V70 FT-IR spectrophotometer. ^1H NMR spectra of HL was acquired with Bruker AV400 NMR instrument in DMSO- d_6 solution with TMS as internal standard. The UV spectra were recorded on a Purkinje General TU-1800 spectrophotometer. The interactions between the complexes and ct-DNA are measured by using literature method^[5] via emission spectra on a Varian CARY Eclipse spectrophotometer.

1.2 Preparations of HL, complexes 1 and 2

As shown in Scheme 1, the ligand HL was produced by condensation of 2-aceto-3-methylpyrazine (1.36 g, 0.01 mol) and benzoylhydrazide (1.36 g, 0.01 mol) in ethanol solution (30 mL) with continuous stirring at room temperature for 3 h. Yield: 2.08 g (82%). Elemental analysis Calcd. for $\text{C}_{14}\text{H}_{14}\text{N}_4\text{O}$ (%): C: 66.13; H: 5.55; N: 22.03. Found (%): C: 66.28; H: 5.44; N: 21.99. FT-IR (cm^{-1}): $\nu(\text{C}=\text{O})$ 1 685, $\nu(\text{C}=\text{N})_{\text{imine}}$

1 582, $\nu(\text{C}=\text{N})_{\text{pyrazine}}$ 1 542. ^1H NMR (400 MHz, DMSO- d_6): δ 10.97 (1H, s, NH), 8.52 (2H, s, pyrazine-H), 7.91 (2H) and 7.53~7.60 (3H) for phenyl-H, 2.80 (3H, s, CH_3), 2.43 (3H, s, CH_3).

The complexes **1** and **2** were generated by reaction of the ligand HL (5 mmol) with equimolar of NiSO_4 or CuSO_4 in methanol solution (10 mL) at room temperature for 1 h. Crystals suitable for X-ray diffraction analysis were obtained by evaporating the corresponding reaction solutions at room temperature.

1: Brown blocks. Anal. Calcd. for $\text{C}_{31}\text{H}_{39}\text{N}_8\text{O}_7\text{S}_{0.5}\text{Ni}$ (%): C: 52.41; H: 5.53; N: 15.77. Found (%): C: 52.30; H: 5.64; N: 15.54. FT-IR (cm^{-1}): $\nu(\text{C}=\text{O})$ 1 654, $\nu(\text{C}=\text{N})$ 1 562, $\nu(\text{C}=\text{N})_{\text{pyrazine}}$ 1 532.

2: Green blocks. Anal. Calcd. for $\text{C}_{29.5}\text{H}_{32}\text{N}_8\text{O}_{7.5}\text{SCu}_2$ (%): C: 45.55; H: 4.15; N: 14.41. Found (%): C: 45.41; H: 4.28; N: 14.32. FT-IR (cm^{-1}): $\nu(\text{C}=\text{O})$ 1 652, $\nu(\text{C}=\text{N})$ 1 560, $\nu(\text{C}=\text{N})_{\text{pyrazine}}$ 1 535.

1.3 X-ray crystallography

The X-ray diffraction measurement for **1** (size: 0.20 mm×0.20 mm×0.20 mm) and **2** (size: 0.15 mm×0.14 mm×0.12 mm) were performed on a Bruker SMART APEX II CCD diffractometer equipped with a graphite monochromatized Mo $K\alpha$ radiation ($\lambda =$

0.071 073 nm) using φ - ω scan mode. Semi-empirical absorption correction was applied to the intensity data using the SADABS program^[10]. The structures were solved by direct methods and refined by full matrix least-square on F^2 using the SHELXTL-97 program^[11]. All non-hydrogen atoms were refined anisotropically. The H atoms of disordered methanol molecule

(occupancy value of each atom being 0.5) in **2** were not added. All the other H atoms were positioned geometrically and refined using a riding model. Details of the crystal parameters, data collection and refinements for **1** and **2** are summarized in Table 1.

CCDC 1876785: **1**; 1876789: **2**.

Table 1 Crystal data and structure refinement for complexes **1** and **2**

	1	2
Empirical formula	C ₃₁ H ₃₉ N ₈ O ₇ S _{0.5} Ni	C _{29.5} H ₃₂ N ₈ O _{7.5} SCu ₂
Formula weight	710.44	777.77
T / K	296(2)	293(2)
Crystal system	Monoclinic	Triclinic
Space group	$C2/c$	$P\bar{1}$
a / nm	2.066 0(3)	1.070 2(5)
b / nm	1.451 20(17)	1.172 3(6)
c / nm	2.273 1(3)	1.420 9(6)
$\alpha / (^\circ)$		71.701(8)
$\beta / (^\circ)$	104.518(2)	73.328(7)
$\gamma / (^\circ)$		72.022(7)
V / nm^3	6.597 6(15)	1.573 8(13)
Z	8	2
$D_c / (g \cdot cm^{-3})$	1.431	1.641
Absorption coefficient / mm^{-1}	0.679	1.481
$F(000)$	2 984	798.0
Reflection collected	16 533	8 031
Unique reflection	5 802	5 486
R_{int}	0.026 0	0.056 2
Goodness-of-fit (GOF) on F^2	1.037	1.070
R indices [$I > 2\sigma(I)$]	$R_1=0.046$ 9, $wR_2=0.130$ 1	$R_1=0.050$ 1, $wR_2=0.139$ 8
R indices (all data)	$R_1=0.055$ 6, $wR_2=0.137$ 7	$R_1=0.066$ 9, $wR_2=0.151$ 0

2 Results and discussion

2.1 Crystal structure description

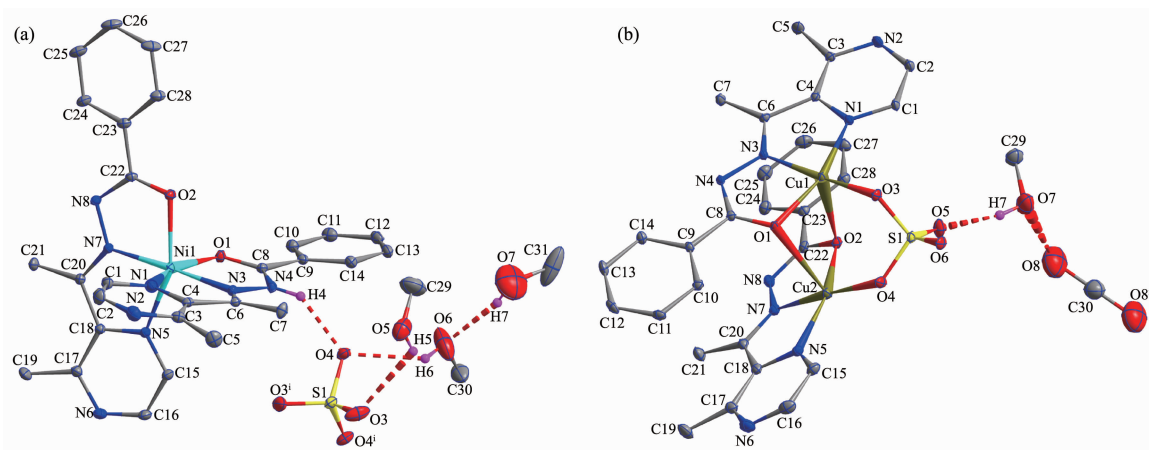
Diamond drawings of complexes **1** and **2** are shown in Fig.1. Selected bond distances and angles are listed in Table 2. As shown in Fig.1a, the asymmetric unit of **1** contains one discrete cationic Ni(II) ion, a half of sulfate anions for charge balance, and three lattice methanol molecules. The center Ni(II) ion with a distorted octahedron geometry is coordinated by two acylhydrazones with [ONN] donor set. It should be noted that one of the acylhydrazone ligands is neutral, since the bond length of C8-O1 (0.123 3(3) nm) is

clearly shorter than that of C22-O2 (0.126 5(4) nm). In the solid state, intermolecular N-H \cdots O (N4-H4 \cdots O4, with D \cdots A distance being 0.270 0(3) nm, D-H \cdots A angle being 139.6 $^\circ$) and O-H \cdots O (O7-H7 \cdots O6, with D \cdots A distance being 0.278 0(12) nm, D-H \cdots A angle being 159.6 $^\circ$; O5-H5 \cdots O3, with D \cdots A distance being 0.296 1(8) nm, D-H \cdots A angle being 118.8 $^\circ$; O6-H6 \cdots O4, with D \cdots A distance being 0.281 5(7) nm, D-H \cdots A angle being 125.0 $^\circ$) hydrogen bonds are helpful to stabilize the crystal structure (Fig.1a).

Complex **2** crystallizes in the triclinic space group $P\bar{1}$ with one discrete dimeric Cu(II) unit in the unit cell. As illustrated in Fig.1b, two Cu(II) ions of

the dimer are separated by 0.317 4 nm and doubly bridged by two O atoms from two acylhydrazone ligands to form a nearly planar four-membered Cu_2O_2 core (r.m.s. deviation: 0.030 15 nm). Each of the Cu(II) ions is also coordinated by two N atoms from one L⁻ ligand (bond length of C8-O1 and C22-O2 are 0.128 8(5) and 0.129 2(5) nm, respectively) and one O atom from the $\eta_2\text{-SO}_4^{2-}$ at the outer axial sites,

giving a distorted square pyramid coordination geometry ($\tau=0.185$ and 0.262 for Cu1 and Cu2, respectively)^[12]. The O-H \cdots O (O7-H7 \cdots O5, with D \cdots A distance being 0.272 4 (7) nm, D-H \cdots A angle being 168.3° ; O8 \cdots O7, with D \cdots A distance being 0.257 4 nm) hydrogen bonds are also present in the crystal (Fig.1b).



Hydrogen bonds shown in dashed line; H atoms of C-H bonds are omitted for clarity; Symmetry codes: ⁱ $-x, y, 1.5-z$; ⁱⁱ $3-x, -y, -z$

Fig.1 Diamond drawings of **1** (a) and **2** (b) with 10% thermal ellipsoids

Table 2 Selected bond lengths (nm) and angles ($^\circ$) in complexes **1** and **2**

1					
Ni1-N1	0.207 5(3)	Ni1-N3	0.199 0(2)	Ni1-O1	0.209 9(2)
Ni1-N5	0.207 4(2)	Ni1-N7	0.195 2(2)	Ni1-O2	0.205 3(2)
N3-Ni1-N1	76.53(9)	N3-Ni1-N5	100.20(10)	N5-Ni1-N1	94.21(9)
N7-Ni1-N1	101.88(10)	N7-Ni1-N3	177.60(9)	N7-Ni1-N5	78.06(9)
N1-Ni1-O1	153.44(9)	N3-Ni1-O1	77.14(8)	N3-Ni1-O2	103.90(9)
N5-Ni1-O1	93.79(9)	N7-Ni1-O1	104.54(9)	N7-Ni1-O2	77.94(9)
O2-Ni1-N1	94.18(9)	O2-Ni1-N5	155.72(9)	O2-Ni1-O1	88.76(8)
2					
Cu1-N1	0.198 7(3)	Cu1-N3	0.190 3(3)	Cu2-N5	0.199 0(4)
Cu2-N7	0.189 7(4)	Cu1-O1	0.195 6(3)	Cu1-O2	0.255 8(3)
Cu1-O3	0.189 4(3)	Cu2-O1	0.258 3(3)	Cu2-O2	0.195 4(3)
Cu2-O4	0.188 3(3)				
N1-Cu1-O2	97.19(12)	N3-Cu1-N1	79.85(14)	N5-Cu2-O1	96.39(12)
N3-Cu1-O1	80.86(12)	N3-Cu1-O2	91.74(12)	N7-Cu2-O2	80.30(14)
N7-Cu2-N5	79.98(16)	N7-Cu2-O1	91.64(13)	O2-Cu2-N5	160.26(14)
O1-Cu1-N1	160.70(13)	O1-Cu1-O2	84.03(11)	O3-Cu1-N3	171.81(14)
O2-Cu2-O1	83.39(11)	O3-Cu1-N1	101.01(14)	O4-Cu2-N5	97.72(15)
O3-Cu1-O1	98.00(13)	O3-Cu1-O2	96.21(12)	O4-Cu2-O2	102.01(14)
O4-Cu2-N7	175.98(14)	O4-Cu2-O1	91.89(13)		

2.2 IR spectra

The FT-IR spectral regions for both complexes were more or less similar due to the similar coordination modes of the ligands. The $\nu(\text{C}=\text{O})$, $\nu(\text{C}=\text{N})_{\text{imine}}$ and $\nu(\text{C}=\text{N})_{\text{pyrazine}}$ bands were at 1 663, 1 578 and 1 559 cm^{-1} , respectively. They shifted to lower frequency values in the IR spectra of complexes, indicating that the carbonyl O, imine N and pyrazine N atoms take part in the coordination^[5]. It is in accordance with the crystal structure study.

2.3 UV spectra

The UV spectra of the ligand HL, **1** and **2** in CH_3OH solution ($10 \mu\text{mol}\cdot\text{L}^{-1}$) were measured at room temperature (Fig.2). The spectra of HL featured two main band at around 230 nm ($\varepsilon=10\,950 \text{ L}\cdot\text{mol}^{-1}\cdot\text{cm}^{-1}$) and 290 nm ($\varepsilon=15\,423 \text{ L}\cdot\text{mol}^{-1}\cdot\text{cm}^{-1}$), which could be assigned to characteristic $\pi-\pi^*$ transition of pyrazine and imine units, respectively^[13]. In the spectrum of complex **1**, these two bands red-shifted to 256 nm ($\varepsilon=12\,832 \text{ L}\cdot\text{mol}^{-1}\cdot\text{cm}^{-1}$) and 306 nm ($\varepsilon=15\,191 \text{ L}\cdot\text{mol}^{-1}\cdot\text{cm}^{-1}$), respectively. By contrast, two bands of the ligand were merged into one at 271 nm ($\varepsilon=17\,968 \text{ L}\cdot\text{mol}^{-1}\cdot\text{cm}^{-1}$) in the spectrum of complex **2**. Moreover, new peaks at 400 nm ($\varepsilon=15\,314 \text{ L}\cdot\text{mol}^{-1}\cdot\text{cm}^{-1}$) and 401 nm ($\varepsilon=12\,955 \text{ L}\cdot\text{mol}^{-1}\cdot\text{cm}^{-1}$) were observed in the

spectra of complexes **1** and **2**, respectively, primarily due to the ligand-to-metal charge transfer (LMCT)^[14]. This indicates that an extended conjugation forms in anionic ligand after complexation.

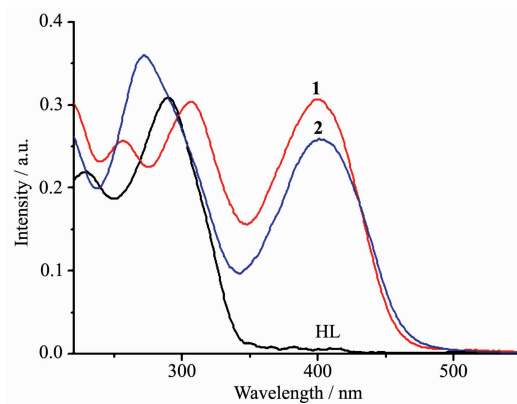
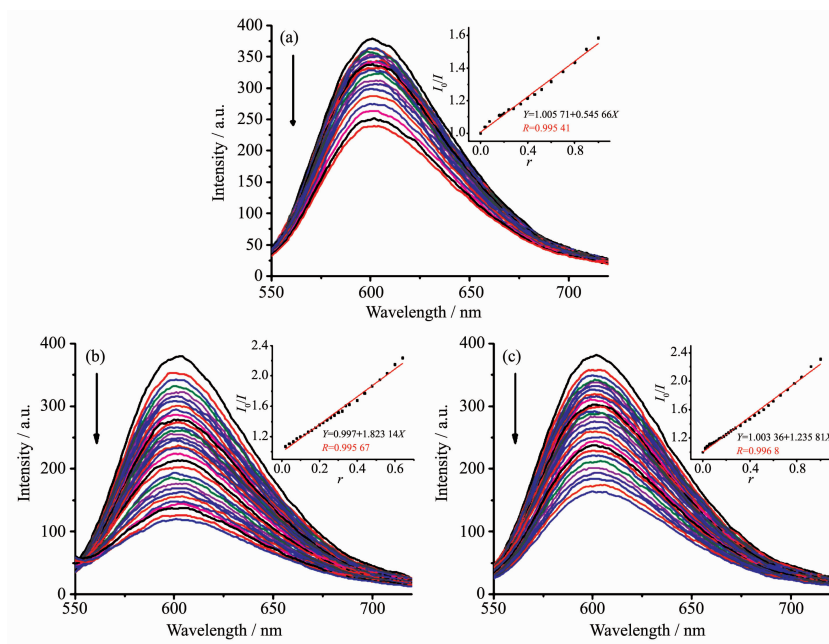


Fig.2 UV spectra of the ligand HL, complexes **1** and **2** in CH_3OH solution at room temperature

2.4 EB-DNA binding study by fluorescence spectrum

It is well known that EB can intercalate nonspecifically into DNA, which causes it to fluoresce strongly. Competitive binding of other drugs to DNA and EB will result in displacement of bound EB and a decrease in the fluorescence intensity^[14-15]. The effects of the ligand and complexes on the fluorescence spectra of EB-DNA system are presented in Fig.3.



Arrow shows the fluorescence intensities change of EB-DNA system upon increasing tested compound concentration; Inset: plot of I_0/I versus r

Fig.3 Emission spectra of EB-DNA system in the absence and presence of ligand HL (a), complexes **1** (b) and **2** (c)

The fluorescence intensities of EB bound to ct-DNA at about 600 nm showed remarkable decreasing trends with the increasing concentration of the tested compounds, indicating that some EB molecules are released into solution after the exchange with the compounds. The quenching of EB bound to DNA by the compounds is in agreement with the linear Stern-Volmer equation: $I_0/I=1+K_{\text{sv}}r^{[14-15]}$, where I_0 and I represent the fluorescence intensities in the absence and presence of quencher, respectively, K_{sv} is the linear Stern-Volmer quenching constant, r is the ratio of the concentration of quencher and DNA. In the quenching plots of I_0/I versus r , K_{sv} values are given by the slopes. The K_{sv} values were 0.545, 1.823 and 1.236 for the ligand HL, complexes **1** and **2**, respectively. The results indicate that interaction of the complexes to DNA is stronger than that of the ligand HL, because the complexes have higher rigidity to bind the base pairs along DNA, thus increasing their binding abilities.

3 Conclusions

Two complexes with a pyrazine-containing benzoylhydrazone ligand were prepared and characterized by single-crystal X-ray crystallography. In complex **1**, the center Ni(II) ion is surrounded by two acylhydrazones with [ONN] donor set, giving a distorted octahedron geometry. By contrast, complex **2** contains one discrete dimeric Cu(II) unit in the unit cell. Moreover, the fluorescence spectra indicated that the interaction of the complexes to DNA is stronger than that of the ligand HL. Further research is needed to better determine the relationship between structures and activities.

References:

- [1] Sönmez M, Sogukomerogullari H G, Öztemel F, et al. *Med. Chem. Res.*, **2014**,**23**:3451-3457
- [2] Hameed A, Al-Rashida M, Uroos M, et al. *Expert Opin. Ther. Pat.*, **2017**,**27**:1-17
- [3] Shanty A A, Philip J E, Sneha E J, et al. *Bioorg. Med. Chem.*, **2016**,**70**:67-73
- [4] Castiñeiras A, García-Santos I, Nogueiras S, et al. *J. Mol. Struct.*, **2014**,**1074**:1-18
- [5] HOU Xu-Feng(侯旭锋), ZHAO Xiao-Lei(赵晓雷), ZHANG Lu(张露), et al. *Chinese J. Inorg. Chem.*(无机化学学报), **2018**,**34**(1):201-205
- [6] Olczak A, Gówka M L, Goka J, et al. *J. Mol. Struct.*, **2007**, **830**:171-175
- [7] Popov L D, Levchenkov S I, Shcherbakov I N, et al. *Russ. J. Coord. Chem.*, **2016**,**42**:151-156
- [8] Bi X, Sun J, Liu W L, et al. *J. Inclusion Phenom. Macrocyclic Chem.*, **2014**,**80**:235-242
- [9] Meira C S, Filho J M D S, Sousa C C, et al. *Bioorg. Med. Chem.*, **2018**,**26**:1971-1985
- [10] Sheldrick G M. *SADABS*, University of Göttingen, Germany, **1996**.
- [11] Sheldrick G M. *SHELX-97, Program for the Solution and the Refinement of Crystal Structures*, University of Göttingen, Germany, **1997**.
- [12] Golovnev N N, Molokeev M S, Sterkhova I V, et al. *Inorg. Chem. Commun.*, **2018**,**97**:88-92
- [13] Kubo T, Shimizu A, Sakamoto M, et al. *Angew. Chem. Int. Ed.*, **2010**,**117**:6722-6726
- [14] MAO Pan-dong(毛盼东), ZHAO Xiao-Lei(赵晓雷), SHAO Zhi-Peng(邵志鹏), et al. *Chinese J. Inorg. Chem.*(无机化学学报), **2017**,**33**(5):890-896
- [15] LIN Long(林龙), LI Xian-Hong(李先宏), ZHANG Bo(张波), et al. *Chinese J. Inorg. Chem.*(无机化学学报), **2017**,**33**(1): 143-148